AFRL-RX-WP-TP-2009-4133

STRESS RATIO EFFECTS ON SMALL FATIGUE CRACK GROWTH IN Ti-6Al-4V (PREPRINT)

M.J. Caton, R. John, W.J. Porter, and M.E. Burba

Metals Branch
Metals, Ceramics and NDE Division

NOVEMBER 2008

AIR FORCE RESEARCH LABORATORY
MATERIALS AND MANUFACTURING DIRECTORATE
WRIGHT-PATTERSON AIR FORCE BASE, OH 45433-7750
AIR FORCE MATERIEL COMMAND
UNITED STATES AIR FORCE

REPORT DOCUMENTATION PAGE

Form Approved
OMB No. 0704-0188

1. REPORT DATE *(DD-MM-YY)*	2. REPORT TYPE	3. DATES COVERED *(From - To)*
November 2008	Journal Article Preprint	01 November 2008 – 01 November 2008

4. TITLE AND SUBTITLE
STRESS RATIO EFFECT ON SMALL FATIGUE CRACK GROWTH IN Ti-6Al-4V (PREPRINT)

5a. CONTRACT NUMBER
In-house

5b. GRANT NUMBER

5c. PROGRAM ELEMENT NUMBER
62102F

6. AUTHOR(S)
M.J. Caton and R. John (AFRL/RXLMN)
W.J. Porter (University of Dayton Research Institute)
M.E. Burba (Central State University)

5d. PROJECT NUMBER
4347

5e. TASK NUMBER
RG

5f. WORK UNIT NUMBER
M02R3000

7. PERFORMING ORGANIZATION NAME(S) AND ADDRESS(ES)

Metals Branch (RXLMN)
Metals, Ceramics and NDE Division
Materials and Manufacturing Directorate
Wright-Patterson Air Force Base, OH 45433-7750
Air Force Materiel Command, United States Air Force

University of Dayton Research Institute
Dayton, OH 45469-0020

Central State University
Wilberforce, OH 45384

8. PERFORMING ORGANIZATION REPORT NUMBER
AFRL-RX-WP-TP-2009-4133

9. SPONSORING/MONITORING AGENCY NAME(S) AND ADDRESS(ES)
Air Force Research Laboratory
Materials and Manufacturing Directorate
Wright-Patterson Air Force Base, OH 45433-7750
Air Force Materiel Command
United States Air Force

10. SPONSORING/MONITORING AGENCY ACRONYM(S)
AFRL/RXLMN

11. SPONSORING/MONITORING AGENCY REPORT NUMBER(S)
AFRL-RX-WP-TP-2009-4133

12. DISTRIBUTION/AVAILABILITY STATEMENT
Approved for public release; distribution unlimited.

13. SUPPLEMENTARY NOTES
To be submitted to International Journal of Fatigue
PAO Case Number and clearance date: 88ABW-2008-0924, 12 November 2008.

14. ABSTRACT
A systematic study of the effects of stress ratio on small fatigue crack growth in Ti-6Al-4V was conducted. Cylindrical fatigue specimens were tested axially at room temperature under a maximum stress of 690 MPa and with stress ratios (R) of 0.5, 0.1, and -1. Tests were periodically interrupted and a standard replication technique was used to monitor the growth of cracks artificially initiated from 30 to 40 μm micro-notches, which were milled into the specimen surface with a focused ion beam (FIB). Measurement of striation spacing from fracture surfaces was evaluated for determining small crack growth rates and showed good agreement with replication data, but is only possible for relatively high stress intensity factor ranges, ΔK, on the order of 10 MPa$\sqrt{m}$ or greater. A significant small crack effect is observed in this alloy, consistent with previous observations, where small cracks grew at stress intensity factor ranges below the long crack threshold and at higher rates than long cracks for equivalent ΔK levels.

15. SUBJECT TERMS
Fatigue; Small crack; Stress ratio; Titanium; Propagation

16. SECURITY CLASSIFICATION OF:			17. LIMITATION OF ABSTRACT:	18. NUMBER OF PAGES	19a. NAME OF RESPONSIBLE PERSON (Monitor)
a. REPORT	b. ABSTRACT	c. THIS PAGE			James M. Larsen
Unclassified	Unclassified	Unclassified	SAR	32	19b. TELEPHONE NUMBER *(Include Area Code)* N/A

Standard Form 298 (Rev. 8-98)
Prescribed by ANSI Std. Z39-18

Stress Ratio Effects on Small Fatigue Crack Growth in Ti-6Al-4V

M. J. Caton[a*], R. John[a], W. J. Porter[b], M. E. Burba[c]

[a] *Materials and Manufacturing Directorate, Air Force Research Laboratory (AFRL/RXLMN), Wright-Patterson AFB, OH 45433-7817, USA*

[b] *University of Dayton Research Institute, Dayton, OH 45469-0020, USA*

[c] *Central State University, Wilberforce, OH 45384, USA*

Abstract

A systematic study of the effects of stress ratio on small fatigue crack growth in Ti-6Al-4V was conducted. Cylindrical fatigue specimens were tested axially at room temperature under a maximum stress of 690 MPa and with stress ratios (R) of 0.5, 0.1, and -1. Tests were periodically interrupted and a standard replication technique was used to monitor the growth of cracks artificially initiated from 30 to 40 μm micro-notches, which were milled into the specimen surface with a focused ion beam (FIB). Measurement of striation spacing from fracture surfaces was evaluated for determining small crack growth rates and showed good agreement with replication data, but is only possible for relatively high stress intensity factor ranges, ΔK, on the order of 10 MPa√m or greater. A significant small crack effect is observed in this alloy, consistent with previous observations, where small cracks grew at stress intensity factor ranges below the long crack threshold and at higher rates than long cracks for equivalent ΔK levels. While a modest effect of stress ratio is seen on small crack growth rates when plotted as a function of crack size (faster growth at lower mean stresses for a given maximum stress), no discernable effect of R is seen when plotting as a function of ΔK. Significant scatter is observed in the small crack growth rates, and the implications of data reduction methods are discussed.

Keywords: Fatigue; Small crack; Stress ratio; Titanium; Propagation

1. Introduction

Turbine engine components can be subjected to variable amplitude loading sufficient to initiate and propagate fatigue cracks and ultimately cause catastrophic failure. One application of particular interest is the high cycle fatigue (HCF) loading of fan and compressor airfoils that occurs during brief sweeps through resonant modes during throttle transients [1]. During these brief resonant excitations, isolated regions of an airfoil will experience a bloom of progressively increasing then decreasing stress amplitude, where the stress ratio (R) is continuously changing (except for the case where R = -1). In determining safe-life limits for components and in developing real-time prognosis systems [2], it is necessary to understand the effect of stress ratio on fatigue crack propagation. In addition, it has been well established that small fatigue crack growth behavior is often poorly represented by traditional long crack data [3] and frequently

demonstrates significantly greater variability than long cracks [4]. Therefore, it is critical that the influence of stress ratio on early crack growth behavior is understood, when crack sizes range from the order of microstructural initiating features up to roughly 1 mm. This paper examines the behavior of small cracks under different stress ratios in Ti-6Al-4V, an alloy commonly used for fan airfoils.

The effect of stress ratio on the long crack behavior in Ti-6Al-4V has been studied quite thoroughly [5-7], much of the work resulting from the Air Force-sponsored *High Cycle Fatigue* initiative [8]. In general, it is observed that crack growth rates for a given stress intensity factor range (ΔK) increase with increasing stress ratio, and crack growth thresholds (ΔK_{th}) decreases with increasing stress ratio. Below a critical stress ratio, R_c, crack closure is seen to be a dominant mechanism controlling the effect of R on crack growth rate. R_c for Ti-6Al-4V is roughly 0.5 [5]. Roughness-induced crack closure (RICC) is reported to be of particular importance in Ti-6Al-4V [7, 9]. For stress ratios greater than R_c, where crack closure is considered negligible, Boyce and Ritche [5] have shown that ΔK_{th} continues to decrease with increasing R and suggest that the K_{max} effect on the intrinsic crack growth mechanism controls this dependence.

Since small fatigue cracks are often considered to experience negligible levels of crack closure compared to long cracks, and closure is thought to be a dominant source of the observed R effect in long crack data, it might be reasonable to assume that small cracks will not demonstrate a significant dependence on R. However, a significant effect of R on small crack growth rates has been reported for aluminum alloys. Caton [10] observed a substantial effect of R on small cracks in a cast 319 aluminum alloy, where small cracks at R = 0.1 grew an order of magnitude faster than those at R = 0.5, and an order of magnitude slower than those at R = -1. Additionally, Newman and Edwards [11] reported a strong stress level effect on the small crack growth rates in a 2024-T3 aluminum alloy that depended upon stress ratio. The stress level effect was most pronounced for negative R values, smaller for R = 0, and no stress level effect was observed at positive R values. While the mechanisms responsible for these observations are not fully understood, it is clearly important to identify the degree to which small crack behavior is influenced by R in order to accurately predict fatigue life under variable amplitude loading applications.

There have been numerous studies of small fatigue crack growth in Ti-6Al-4V [8, 12-15], where several stress ratios have been examined. Fig. 1 shows a compilation of these data sets. Included in Fig. 1 are long crack growth curves, which were tabulated from a series of data generated under the HCF Initiative [16]. The influence of stress ratio on the long crack growth is consistent with that described above. Higher applied R results in faster crack growth rates and lower ΔK_{th}, and the effect is less pronounced at higher R values (0.5 versus 0.8), where the contribution of crack closure is greatly diminished. The small crack data in Fig.1 indicates a significant amount of scatter in behavior and provides clear evidence of a small crack effect in this alloy. That is, small cracks are observed to grow at ΔK levels below the long crack threshold (ΔK_{th}) and at faster rates than that of long cracks for a given ΔK. Within the small crack data provided in Fig. 1, which were acquired at stress ratios ranging from -1 to 0.5, it is difficult to discern any clear influence of stress ratio. However, it is important to note that the individual sets of small crack data were acquired under disparate testing conditions and for

slightly different Ti-6Al-4V alloys; therefore direct comparison of these data is somewhat tenuous. Table 1 summarizes some of the key details of these tests and indicates where differences exist that could influence the crack growth behavior and render direct comparisons for different stress ratios inappropriate. While it is quite possible that stress ratio will have little influence on small crack growth in this alloy at room temperature, it is difficult to conclusively deduce this fact strictly from the data available in the literature.

Table 1
Summary of test details for numerous small crack studies in Ti-6Al-4V alloys with bi-modal microstructures [8, 12-14]. Crack growth data are shown in Fig. 1.

Reference	Alloy	σ_{yield} *(MPa)*	R	σ_{max} *(MPa)*	Crack Sizes *(μm)*	Initiation
Gallagher et al. [8]	Ti-6Al-4V 60% α_p	930	0.1	613	5 – 200	Natural initiation
			0.5	759	5 – 200	Natural initiation
Peters et al. [12]	Ti-6Al-4V 60% α_p	915	0.1	550	50 – 1,500	Natural initiation at R = -1, 650 MPa to crack size of ~50 μm
Hines and Lutjering [13]	Ti-6Al-4V 35% α_p	940	-1	350	75 – 1,100	Natural initiation at R = -1, 650 MPa to crack size of ~75 μm
			-1	650	75 – 1,100	Natural initiation at R = -1, 650 MPa
Jin et al. [14]	Ti-6Al-4V % α_p not reported	907	0.4	249 to 305	5 – 600	Natural initiation

This study is aimed at conducting a systematic examination of the effect of stress ratio on small fatigue crack growth rates in a controlled microstructure of Ti-6Al-4V [8]. In addition, the degree of variability observed in small crack behavior is evaluated and the sensitivity to different data reduction methods is explored. Determination of small crack growth rates based upon the measurement of striation spacing from fracture surfaces is evaluated similar to the work of Lenets and Bellows [15]. Growth rates from striation spacing shows good agreement with replication data, but is only applicable for relatively high stress intensity factor ranges where ΔK is on the order of 10 MPa$\sqrt{m}$ or greater.

2. Experimental procedures

The material investigated in this study is a Ti-6Al-4V alloy in a solution-treated and over-aged (STOA) condition. The specimens tested were taken from the same lot of material used in the Air Force-sponsored *High Cycle Fatigue* initiative [8], which included numerous industry,

university, and government researchers. The microstructure, shown in Fig. 2, consists of 60-vol% equiaxed primary alpha phase with an average grain size of 20 μm and 40-vol% transformed beta phase. The alloy demonstrates average yield strength of 930 MPa and ultimate tensile strength of 978 MPa at room temperature. Fig. 2 (a) shows that the grain structure is quite equiaxed and uniform, and Fig. 2 (b) provides an alpha grain size distribution acquired through orientation image mapping (OIM) software. It is seen that the average alpha grain size is roughly 10 μm.

The dimensions of the smooth, cylindrical specimen used to monitor small fatigue crack growth are shown in Fig. 3. The gage section is 20.6 mm long and has a diameter of 4.2 mm. Micro-notches were milled into the specimens using a focused ion beam (FIB) in order to artificially initiate fatigue cracks. Each specimen contained 9 micro-notches and Fig. 4 shows that they were placed an adequate distance from each other in order to minimize crack interaction effects. Fig. 5 shows an example of a micro-notch as seen both on the specimen surface and on the fracture surface. All micro-notches had a depth to surface length ratio of 1 to 2, and a height to surface length ratio of roughly 1 to 10. The surface lengths of the micro-notches used are outlined in Table 2, and were roughly 30 μm or 40 μm depending on the testing condition.

Small crack growth was monitored using a standard replication technique with cellulose acetate tape. Fatigue cycling was periodically interrupted, and replicas were taken while placing the specimen under a tensile hold load of 60% σ_{max}. All tests were conducted using a servo-hydraulic test frame under load-control at room temperature in lab air and at a frequency of 20 Hz. Four specimens were tested in total. Three specimens were tested at a maximum stress of 690 MPa with stress ratios of -1, 0.1, and 0.5, respectively. Additionally, one specimen was tested at a stress ratio of 0.1 with a maximum stress of 620 MPa. Subsequent to failure, the fracture surface of each specimen was examined with scanning electron microscopy (SEM). For each specimen tested at 690 MPa, fatigue striations were found and the average striation spacing was measured for numerous crack sizes using Fovea Pro, an image analysis software package.

3. Results and discussion

3.1 Crack Initiation

While each fatigue specimen contained 9 micro-notches, a crack did not necessarily initiate from every micro-notch. Table 2 summarizes the observations of crack initiation in each of the specimens. Most of the micro-notches were 30 μm in surface length, however, 6 of the 9 micro-notches in the specimen tested at R = 0.5 were made somewhat larger (40 μm) since it was expected that initiating a crack would be more challenging under these loading conditions. Included in Table 2 are initial stress intensity ranges, ΔK, calculated using the solution from Raju and Newman [17] for a surface crack in a rod. These calculations assume that the micro-notches are semi-circular cracks (a = c) like that depicted in Fig. 4. It is recognized that this assumption simplifies the true stress intensity factor at the micro-notch tips; however, these values provide a very reasonable measure of the relative crack driving force from these artificial flaws under the different loading conditions. It should be noted that for the specimen tested at R = -1, only the

tensile portion of the loading was included in the calculation of ΔK. In all cases, except for the analysis of striation spacing measurements, ΔK was calculated for the crack front at the surface of the specimen. For all ΔK calculations shown in the paper, a semicircular crack shape is assumed, where the crack depth (a) is assumed to be equivalent to half the crack surface length (c).

Table 2
Summary of test conditions and the number of cracks observed to initiate from FIB-milled micro-notches.

Specimen ID	σ_{max} *(MPa)*	R	Number of Micro-Notches	Notch Length *(μm)*	Initial ΔK *(MPa √m)*	Cracks Initiated
02-040	690	-1	9	30	3.45*	9
02-049	690	0.1	9	30	3.11	8
02-042	620	0.1	9	30	2.79	1
02-038	690	0.5	6	40	1.79	1
			3	30	1.55	0

**Only the tensile portion of the loading is included in the ΔK calculation at R = -1.*

It is seen in Table 2 that the number of micro-notches from which cracks initiated decreases with decreasing ΔK. A significant reduction in the percentage of micro-notches producing fatigue cracks is observed between the specimens tested at maximum stresses of 690 and 620 MPa with R = 0.1. At 690 MPa, 8 of the 9 micro-notches produced fatigue cracks, while only 1 of the 9 micro-notches produced fatigue cracks at 620 MPa. The calculated ΔK values for the micro-notches in these specimens are 3.11 and 2.79 MPa√m, respectively. The observations in Table 2 suggest that a statistical small-crack threshold, ΔK_{th}, for this alloy exists at roughly 3 MPa√m. That is, looking strictly at the initial ΔK values in Table 2 and ignoring R, the data suggest that if a micro-notch has an associated ΔK greater than 3 MPa√m then a crack will almost certainly initiate and grow, but if the ΔK is less than 3 MPa√m then it is very unlikely that a crack will initiate and grow. This value of 3 MPa√m is close to the long crack threshold reported for this alloy at R = 0.5 and 0.8 shown in Fig. 1 [8, 16]. In addition, this is also consistent with the observation by Ritchie et al. [6] that no FOD-initiated small cracks were observed in Ti-6Al-4V below 2.9 MPa√m. Ritchie et al. [6] also examined the theoretical derivations for intrinsic threshold of Ti-6Al-4V. They calculated an intrinsic threshold of 4.3 MPa√m based on an approach from Sadananda and Shahinian [18], which derives the driving force below which dislocations are no longer emitted from the crack tip. They also calculated an intrinsic threshold of 1 MPa√m based on an approach from Weertman [19], which derives the limiting condition for dislocation emission from an atomically sharp crack. The observations of crack initiation outlined in Table 2 are fairly consistent with these analytical predictions.

The fact that some flaws initiate cracks and some do not under nominally equivalent stress intensity conditions underscores the important role played by the local microstructure in controlling the variability observed in fatigue behavior. Since small fatigue cracks are strongly influenced by the local surrounding microstructure, they demonstrate significantly more scatter in growth behavior than long cracks. Correspondingly, small cracks also demonstrate more scatter in threshold behavior. Therefore, a definitive value of ΔK_{th} derived strictly from mechanics cannot be assigned for small flaws, but rather a range of stress intensities within which the probability of a flaw initiating and growing a fatigue crack will decrease from near 100% to near 0% should be defined through probabilistic methods.

3.2 Effect of Stress Ratio on Small Crack Growth

The crack growth behavior of the critical crack (the most dominant crack that ultimately caused failure) for each specimen tested at 690 MPa is shown in Fig. 6. Based upon the crack size measured from the final replica, the critical crack sizes ranged from roughly 2 to 3 mm for full, surface crack length (2c). As expected, the number of cycles required to reach the failure increased with increasing mean stress. Fig. 6 also shows that the replication technique provided a significant amount of data, where 20 to 60 measurements are available for a given crack. Fig. 7 shows the crack growth rate of the critical crack for each specimen tested at 690 MPa as a function of crack size. Here it is seen that the stress ratio does influence the rate of crack growth, with faster growth resulting from higher applied stress ranges. The crack tested at R = -1 ($\Delta\sigma$ = 1,380 MPa) grew about 1 to 4 times faster than the crack tested at R = 0.1 ($\Delta\sigma$ = 621 MPa), which in turn grew about 2 to 6 times faster than the crack tested at R = 0.5 ($\Delta\sigma$ = 345). When plotted as a function of ΔK, as shown in Fig. 8, any influence of stress ratio on growth rate is difficult to discern. The lack of R effect on small crack growth is, in general, consistent with the available small crack data compiled from the literature and shown in Fig. 1. However, the data in Fig. 8 was obtained under very controlled conditions, where specimen design, alloy source, initiation technique, and maximum stress were all held constant in order to isolate the influence of R.

Fig. 9 shows photos of the dominant cracks grown at the maximum stress of 690 MPa and stress ratios of 0.5, 0.1, and -1. It is seen that the shape of the cracks, as viewed from the specimen surface, are very similar at all stress ratios. The relative roughness or tortuosity of the crack paths was evaluated by measuring the peak-to-peak distance for all of the cracks at a given size (~500 μm), depicted as δ in Fig. 9b. For the three cracks shown in Fig. 9, it appears that stress ratio may have an effect on crack path, where δ was measured to be roughly ~56 μm, ~66 μm, and 104 μm at R of 0.5, 0.1, and -1, respectively. However, after measuring this parameter for all of the small cracks in this study, it is difficult to conclusively state that R influences crack roughness. It was found that δ ranged from 50 to 130 μm at R = -1, from 45 to 100 μm at R = 0.1, and was 56 μm for the single crack observed at R = 0.5. In addition, the roughness of the fracture surfaces was quantitatively evaluated using a 3D microscopy software (MeX by Alicona Imaging GmbH) and no definitive difference was observed at the different stress ratios.

The reason for observing no influence of stress ratio on small crack growth rate in this alloy (Figs. 1 and 8) is not fully understood, but the following discussion offers thoughts on the observation. For long cracks in Ti-6Al-4V, a distinct influence of stress ratio has been reported when plotting growth rates as a function of ΔK, and the effect is attributed primarily to the varying level of crack closure [5-7]. In particular, roughness-induced crack closure (RICC) is considered to be important in this alloy. Dubey et al. [7] showed a marked effect of R on long crack growth in Ti-6Al-4V for R values ranging from 0.02 to 0.8, and demonstrated that this influence of stress ratio was essentially eliminated when plotting the growth rates as a function of the effective stress intensity factor range (ΔK_{eff}), which accounts for closure. Since crack closure levels are often considered to be negligible for small cracks, perhaps the lack of R effect observed in Fig. 8 simply reflects closure-free crack growth where ΔK adequately represents the effective crack driving force.

It is interesting to consider the lack of R effect on small crack growth in Ti-6Al-4V in the context of the behavior of other alloys. For example, Caton [10] observed a profound effect of R on small cracks in a cast 319 aluminum alloy, where growth rates at R = 0.1 were an order of magnitude greater than those at R = 0.5, and an order of magnitude less than those at R = -1. The test conditions applied to the cast aluminum specimens were extremely similar to those used in the current study of Ti-6Al-4V to acquire the data shown in Fig. 8. The stress ratios of 0.5, 0.1, and -1 were investigated for a constant maximum stress of ~76% σ_{yield}. In both studies, small cracks were grown in smooth, axial specimens and ranged in size from roughly 50 μm to 2 mm. It was thought that the considerable effect of R on the small crack behavior in the cast aluminum alloy was due to different levels in RICC. While closure was not measured in this study, there was compelling, qualitative evidence that the crack tip opening displacement was progressively greater for the lower stress ratios where, it was hypothesized, asperities on crack surfaces were being deformed and producing smoothed crack faces. It could also be postulated that the difference in observed effect of R on small crack growth in the Al and Ti alloys is related to the different degree of plasticity ahead of the crack tip in the different alloys. In general, face-centered cubic (FCC) aluminum alloys accommodate easier slip than do hexagonal-close packed (HCP) titanium alloys, contributing to higher levels of plasticity ahead of the crack tip in aluminum. For example, at room temperature the critical resolved shear stress for basal slip {0001} <11-20> in near-pure titanium is approximately 110 MPa and that for the preferred prismatic slip {10-10} <11-20> is approximately 49 MPa [20]. In contrast, the room-temperature critical resolved shear stress for the preferred {111} <110> slip in near-pure aluminum is about 1 MPa [21]. Therefore, it is possible that the degree of plasticity ahead of the crack tip in the cast aluminum alloy is much greater than that in the Ti-6Al-4V alloy, such that the assumption of small scale yielding inherent with the application of ΔK is violated. The plasticity, along with the associated violation of small scale yielding, could be more pronounced the greater the applied stress range, leading to the observed stress ratio effect in cast aluminum.

3.3 Effect of Stress Level on Small Crack Growth

At the stress ratio of R = 0.1, small crack growth rates were monitored at both 620 and 690 MPa, allowing for an examination of the effect of stress level on small crack growth. Fig. 10 compares the small crack growth rates at R = 0.1 for the dominant crack grown at and 690 MPa

and the single crack grown at 620 MPa. It is clearly seen that there is no stress level effect on the growth of these two cracks.

Stress level effects on small crack growth can be very significant and are an indication of the breakdown of ΔK as an appropriate correlating parameter for small cracks. This phenomenon has been reported for numerous alloys [10, 11, 22-24]. The effect of stress level on small crack growth in Ti-6Al-4V was examined previously by both Hines and Lutjering [13] and Jin et al. [14]. Within the scatter of the relatively limited small crack data presented in these two studies, it is difficult to conclusively argue that a stress level effect is present and it appears that the findings of these other studies are consistent with that of Fig. 10.

3.4 Scatter and Data Reduction

It is known that the scatter in small crack growth can be quite significant, particularly when compared to that of long cracks. With the introduction of multiple micro-notches in the fatigue specimens, as shown in Fig. 4, it is possible to examine the growth behavior of numerous cracks using a relatively limited number of tests. The crack size measurements for all of the cracks that initiated from micro-notches at 690 MPa and R of 0.1 and -1 are shown in Fig. 11. It is seen for both specimens that one or two cracks reached a critical size ($2c > \sim 2$ mm) well ahead of the other cracks, where the majority of small cracks have a full surface length, 2c, on the order of 800 μm or less at the time of failure. However, most cracks in these two specimens did demonstrate significant propagation over the life of the specimens. Fig. 12 shows the crack growth rate as a function of ΔK for all of the small cracks that initiated from micro-notches at $\sigma_{max} = 690$ MPa. The scatter in these data can be over an order of magnitude at lower ΔK levels, and reduces as the cracks get larger. For many of the cracks, there are periods of multiple replication examinations that show no growth and the cracks are temporarily arrested, at least at the specimen surface. When this occurs, a crack growth rate of 10^{-7} mm/cycle has been assigned to the crack to represent negligible crack advance on the dc/dN vs. ΔK plot. The data in Fig. 12 also seem to indicate that somewhat faster growth rates are observed at R = -1 at lower ΔK levels when compared to R = 0.1 and 0.5. However, the scatter in the R = -1 data is larger than that at the higher stress ratios, and also shows more temporary arrest of cracks than that seen at R = 0.1 and 0.5. The reason for the larger scatter observed at R = -1 is not understood and it may be an artifact of the amount of data represented. In other words, if more repeat tests were performed, the scatter at the higher stress ratios may begin to match that at R = -1. No conclusions can be drawn about the different levels of scatter at this point.

The variability observed in small crack growth rates is largely due to the strong influence of the local microstructure, where cracks may grow relatively quickly through a favorably oriented grain and then temporarily arrest at hard barriers such as grain boundaries with unfavorably oriented grains. As the crack becomes larger, these disparate influences on growth rate from local regions are averaged out across the crack front and the scatter in growth rates is reduced. While the large scatter in growth behavior for small cracks has a true physical basis, it is important to note that the method used to reduce the crack measurement data can also significantly influence the scatter. Since data like that shown in Fig. 12 can be used to estimate

the safe-life of components, it is worthwhile to examine the sensitivity of this apparent variability to the data reduction methods.

The crack growth rates shown in Fig. 12 were calculated by applying a 3-point sliding polynomial fit to the individual data sets of crack size vs. cycles shown in Figs. 6 and 11. The scatter in the growth rate data will be reduced if a higher number of data points are selected in this method, such as a 5-point or 7-point sliding fit. All of the crack measurements are used in this approach where each successive set of three c-N points are regressed, and temporary crack arrest is captured and represented in the dc/dN vs. ΔK plot. An alternative data reduction method has been presented previously by Larsen et al. [25], whereby a crack extension increment, Δc_{inc} or Δa_{inc}, is used as a criterion for determining the selection of data that will be regressed. This modified incremental polynomial regression method has been applied to the R = -1 data from Fig. 8, where two different levels Δc_{inc} were used. Fig. 13 shows the effect of the different data reduction methods on the dc/dN vs. ΔK curves, and it is seen that the scatter is considerably reduced with the modified incremental regression method, where the crack extension increment of 10 μm is chosen. Note that 10 μm is roughly the average alpha grain size in this Ti-6Al-4V alloy. It is important to recognize that the reduced scatter in the regressed growth rate data can be beneficial by enabling more straightforward life prediction analyses, but it must be further appreciated that this method eliminates some of the indications of true variability in small crack behavior such as temporary crack arrest. The arrest of small cracks is often very brief, however, in some cases such periods of incubation can consume significant fractions of the total fatigue life and neglecting this in life predictions can lead to inaccuracies. It is suggested that the large variability in small crack growth behavior be treated with probabilistic modeling methods [26].

One consideration that was assumed negligible in the small crack growth data analysis, but should be mentioned, is the potential interaction effects that could be operative due to the presence of multiple cracks within a single specimen. As mentioned previously, the placement of the micro-notches shown in Fig. 4 was devised such that the distances between growing fatigue cracks would be maximized, to the extent possible, in order to minimize interactions. However, when a crack is growing on the same axial line of loading as another crack in close proximity, the effective ΔK can be reduced. Isida et al. [27] numerically examined this problem of an array of semi-elliptical surface cracks in a semi-infinite solid under tension. They showed that when the ratio of the distance between adjacent cracks (3 mm in the case of the current study as illustrated in Fig. 4) to the crack depth (c) is greater than roughly 4, then the influence of adjacent cracks on reducing ΔK is nearly negligible. As seen in Fig. 11, the great majority of the crack growth data analyzed in the current study is for crack depths less than 600 μm, where the ratio described above is greater than 5 (i.e., 3 mm / 0.6 mm). However, the few dominant cracks monitored in this study were observed to reach crack depths as large as 1.6 mm, near the end of the fatigue life. The analysis by Isida et al. suggests that the ΔK for adjacent cracks of this size should be approximately 90% that of an isolated crack of the same size in a semi-infinite solid. However, this analysis assumes that the adjacent cracks are both the same size, and in the current study the cracks adjacent to the dominant cracks were significantly smaller in size. So it is quite reasonable to assume that the interaction effects for adjacent cracks are essentially negligible for all of the crack data analyzed in the current study.

3.5 Small Crack Growth from Natural Initiation Sites

For the specimen tested at maximum stress of 690 MPa and stress ratio of -1, some surface cracks were observed to naturally initiate from microstructural features, in addition to the small cracks initiated from the 9 micro-notches. Two of these naturally initiated cracks were measured and the growth rate data is compared to that of the nine small cracks that initiated from the 30 μm micro-notches in Fig. 14. The small crack growth behavior appears to be very similar for cracks emanating from micro-notches and for those initiated from a natural microstructural feature. The size of the naturally initiated cracks was roughly 5 μm in surface length when first detectable on the replication tape. This corresponds to an initial ΔK of 1.4 MPa$\sqrt{m}$, which is about three times lower than that of the cracks initiated from the micro-notches. The data from the naturally initiated cracks further reinforce the small crack effect in this Ti-6Al-4V alloy, and demonstrate growth rate conditions that are fairly consistent with the intrinsic threshold estimates derived theoretically by Ritchie et al. [6] and discussed previously.

3.6 Fractography and Striation Spacing

Fractography was performed on all of the fatigue specimens using scanning electron microscopy (SEM). Most specimens had only a single critical crack apparent on the fracture surface, and it was difficult to discern the crack shape. However, the specimen tested at 690 MPa and R = 0.1 had three cracks on the fracture surface, two of which were sub-critical and provided a very clear indication of crack shape. These two cracks are shown in Fig. 15. The crack depth (a) and surface length (2c) were measured for these two cracks in order to calculate the aspect ratio (a/c). It was found that the crack in Fig. 15a had a depth of 692 μm and an aspect ratio of 1.03, while the crack in Fig. 15b had a depth of 380 μm and an aspect ratio of 1.15. It is thought that the shape of these cracks is reasonably representative of all the small cracks examined in this study and that the assumption of an aspect ratio of 1 used in the ΔK calculations is reasonable.

In addition to evaluating the crack shape, specimens were examined fractographically to identify and measure striations. Striations are a fairly common feature on the fracture surfaces of ductile alloys that indicate the progression of fatigue crack advance. Under certain conditions, it is thought that a striation is created by a single cycle of fatigue loading. If it is further assumed that every cycle creates a striation, then the crack growth rate at a given period of the fatigue life can be deduced by measuring the spacing of the striations. Fig. 16 shows SEM images of striations measured at different crack depths for the specimens tested at 690 MPa and stress ratios of -1, 0.1, and 0.5. The images were taken at depths of 0.3, 0.5, 0.8, and 1.0 mm away from the specimen surface on a direct line between the initiating micro-notch and the center of the specimen. For each of these depths, ΔK was calculated using the solution from Raju and Newman [17] for a surface crack in a rod for the interior location of the crack front. These ΔK values are included with each photo of striations in Fig. 16. It is notable that striations are only evident above a ΔK level of approximately 10 MPa$\sqrt{m}$ in these specimens. This is consistent with the observations of Lenets and Bellows [15], who also studied the striation spacing in Ti-6Al-4V in relation to crack growth rate measurements.

Fig. 17 shows crack growth rate calculations based upon striation spacing measurements as a function of ΔK, in comparison to the crack growth data determined from surface crack measurements using replication. The data from replication measurements are the same as that shown in Fig. 8, with the exception that ΔK has now been calculated for the interior front of the crack rather than the surface. Fig. 17 indicates that the striation spacing appears to provide a very good estimate of crack growth rate under these testing conditions, when compared to surface measurements. This can provide valuable information, particularly for the purposes of failure analysis. However, it is a technique with limitations that must be recognized. For example, Lenets and Bellows [15] did not see any striations in a specimen tested at R = 0.8, which is understandable since ΔK of 10 MPa√m is very close to the critical level to cause fracture at this stress ratio. In addition, the growth rates from striation spacing reported by Lenets and Bellows for ΔK levels greater than ~50 MPa√m were seen to underestimate the growth rates observed from standard long crack growth methods. So while the method of striation spacing measurement can have great utility in elucidating the conditions under which a fatigue failure occurred in the field of service, it is important to recognize the window of loading conditions within which the technique is applicable and the inherent assumptions are valid.

4. Summary and conclusions

A systematic study of the effect of stress ratio on the small crack growth behavior of Ti-6Al-4V was conducted. Cracks were initiated from FIB-milled micro-notches that were 30 to 40 μm in length, and crack propagation was monitored using a standard replication technique. The following conclusions can be drawn:

- Cracks did not initiate from every micro-notch and an average small crack threshold of 2 to 3 MPa√m could be inferred from the data. Most micro-notches did not initiate a crack if ΔK was less than ~3 MPa√m, and no cracks were seen to initiate from a micro-notch where ΔK was less than 1.8 MPa√m.

- At a maximum stress of 690 MPa and stress ratio of -1, a limited number of cracks were observed to initiate naturally from microstructural features. These cracks grew at ΔK levels as low as 1.4 MPa√m, and there was no difference in growth behavior observed between the naturally initiated cracks and those emanating from the micro-notches.

- A small crack effect is evident in the data, where small cracks grew at stress intensity ranges below the long crack threshold and at higher rates than long cracks for equivalent ΔK levels. This is consistent with previous studies of this alloy [8, 12, 13].

- When plotting the small crack data as a function of ΔK, there is no discernable influence of stress ratio on growth rate for the conditions of σ_{max} = 690 MPa and stress ratios of 0.5, 0.1, and -1. It is thought that the diminished role of crack closure, compared to long cracks, plays an important role in the observed lack of R effect. Additionally, the absence of an R effect on the dc/dN vs. ΔK behavior of small cracks in Ti-6Al-4V is notable when compared to the profound R effect reported in other alloys, particularly cast 319 aluminum [10] where 2 orders of magnitude difference in growth rate is observed

between R of 0.5 and -1. It is thought that the degree of plasticity ahead of the small crack tips in Ti-6Al-4V is modest in comparison to that in aluminum alloys, thereby retaining the validity of the small scale yielding assumption inherent in the use of ΔK.

- Fatigue striations were evident over much of the fracture surfaces of the specimens tested in this study. Small crack growth rates estimated from the measurement of striation spacing was shown to be in good agreement with the growth rates determined from surface replication. It is noted, however, that the applicability of this method has limitations; striations are not clearly generated on the fracture surfaces of Ti-6Al-4V below a ΔK of roughly 10 MPa$\sqrt{m}$, and there is evidence from Lenets and Bellows [15] that the growth rates determined from striation spacing underestimates growth rates from standard long crack methods for ΔK levels greater than roughly 50 MPa$\sqrt{m}$.

- The scatter in the small crack growth data was significant, and ranged from over an order of magnitude at ΔK levels less than roughly 10 MPa$\sqrt{m}$ to about 2X at ΔK levels greater than roughly 15 MPa$\sqrt{m}$. The large scatter in measured small crack growth rates is related to the strong influence of the local microstructure. However, the degree of scatter in the data is also a function of the data regression technique used to calculate dc/dN. It is shown that a modified incremental regression technique, which calculates growth rate only when a set level of crack advance is reached (e.g., $\Delta c_{inc} = 10$ μm), can reduce the scatter considerably when compared to a standard 3-pt sliding polynomial regression. It is important to recognize that the modified incremental regression approach can conceal the occurrence of true physical phenomena, such as temporary small crack arrest, that can significantly influence the total fatigue life. Probabilistic methods are likely the best approach for treating the significant variability in small crack behavior.

Acknowledgements

This work was performed at the Air Force Research Laboratory, Materials and Manufacturing Directorate (AFRL/RXLMN), Wright-Patterson Air Force Base, OH. The authors gratefully acknowledge the partial support of Dr. Leo Christodoulou of the Defense Advanced Research Projects Agency (DARPA) under DARPA order S271. W.J. Porter was supported under on-site AF Contract No. FA8650-04-C-5200, and M. E. Burba was supported by the SOCHE (Southwestern Ohio Council for Higher Education) program. The authors also gratefully acknowledge the cooperation of Drs. Youri Lenets and Craig McClung for providing data and testing information generated during the Air Force-sponsored *High Cycle Fatigue* initiative.

References

[1] J. W. Littles, Jr. and M. B. Buczek, "Engine System Prognosis," Materials Damage Prognosis, J. M. Larsen, L. Christodoulou, J. R. Calcaterra, M. L. Dent, M. M. Derriso, W. J. Hardman, J. W. Jones, and S. M. Russ, Eds., TMS (The Minerals, Metals & Materials Society), pp. 23-29, 2005.

[2] L. Christodoulou and J. M. Larsen, “Materials damage prognosis: A revolution in asset management,” Materials Damage Prognosis, J. M. Larsen, L. Christodoulou, J. R. Calcaterra, M. L. Dent, M. M. Derriso, W. J. Hardman, J. W. Jones, and S. M. Russ, Eds., TMS (The Minerals, Metals & Materials Society), pp. 3-10, 2005.

[3] Small Fatigue Cracks: Mechanics, Mechanisms and Applications, K. S. Ravichandran, R. O. Ritchie, and Y. Murakami, (Eds.), Elsevier Science Ltd., Oxford, UK, 1999.

[4] S. K. Jha, M. J. Caton, and J. M. Larsen, " A new paradigm of fatigue variability behavior and implications for life prediction," Materials Science and Engineering, **468-470**, pp. 23-32, 2008.

[5] B. L. Boyce and R. O. Ritchie, "Effect of load ratio and maximum stress intensity on the fatigue threshold in Ti-6Al-4V", Engineering Fracture Mechanics, **68**, pp. 129-147, 2001.

[6] R. O. Ritchie, B. L. Boyce, J. P. Campbell, O. Roder, A. W. Thompson, and, W. W. Milligan, "Thresholds for high-cycle fatigue in a turbine engine Ti-6Al-4V alloy", International Journal of Fatigue, **21**, pp. 653-662, 1999.

[7] S. Dubey, A. B. O. Soboyejo, and W. O. Soboyejo, "An investigation of the effects of stress ratio and crack closure on the micromechanisms of fatigue crack growth in Ti-6Al-4V", Acta Materialia, **45**, pp. 2777-2787, 1997.

[8] J. Gallagher et al., “Advanced high cycle fatigue (HCF) life assurance methodologies,” Air Force Technical Report, AFRL-ML-WP-TR-2005-4102, 2004.

[9] K. S. Ravichandran, "Near threshold fatigue crack growth behavior of a titanium alloy: Ti-6Al-4V", Acta Metall. Mater., **39**, pp. 401-410, 1991.

[10] M. J. Caton, “Predicting fatigue properties of cast aluminum by characterizing small-crack propagation behavior,” Ph.D Dissertation, University of Michigan, Ann Arbor, MI, 2001.

[11] J. C. Newman, Jr. and P. R. Edwards, “Short crack growth behavior in an aluminum alloy – An AGARD cooperative test programme,” AGARD Report # 732, AGARD, 1988.

[12] J. O. Peters, O. Roder, B. L. Boyce, A. W. Thompson, and R. O. Ritchie, "Role of foreign object damage on thresholds for high-cycle fatigue in Ti-6Al-4V", Metallurgical and Materials Transactions A, **31A(6)**, pp. 1571-1583, 2000.

[13] J. A. Hines and G. Lutjering, "Propagation of microcracks at stress amplitudes below the conventional fatigue limit in Ti-6Al-4V", Fatigue Fract. Engng Mater Struct, **22**, pp. 657-665, 1999.

[14] O. Jin, R. W. Hamm, and W. S. Johnson, " Microstructural influences on the growth of small cracks in Ti-6Al-4V", Fatigue Fract. Engng Mater Struct, **25**, pp. 563-574, 2002.

[15] Y. N. Lenets and R. S. Bellows, “Crack propagation life prediction for Ti-6Al-4V based on striation spacing measurements,” International Journal of Fatigue, **22**, pp. 521-529, 2000.

[16] Dr. R. Craig McClung, Southwest Research Institute, Tabulated data generated from the Air Force-sponsored HCF initiative provided through personal communication.

[17] I. S. Raju and J. C. Newman, Jr., “Stress intensity factors for circumferential surface cracks in pipes and rods under tension and bending loads,” Fracture Mechanics: 17th Volume, ASTM STP 905, ASTM, pp. 789-805, 1986.

[18] K. Sadananda and P. P. Shahinian, “Prediction of threshold stress intensity for fatigue crack growth using a dislocation model,” International Journal of Fracture, **13**, pp. 585-594, 1977.

[19] J. Weertman, “Fatigue crack growth in ductile metals,” In: Mechanics of Fatigue, Editor, T. Mura, ASME, pp. 11-19, 1982.

[20] E. A. Anderson, D. C. Jillson, and S. R. Dunbar, “Deformation mechanisms in alpha titanium,” *Trans. AIME*, **197**, pp. 1191-1197, 1953.

[21] F. D. Rosi and C. W. Mathewson, *Trans. AIME*, **188**, 1159, 1950.

[22] H. Nisitani, M. Goto, and N. Kawagoishi, “A small-crack growth law and its related phenomena,” Engineering Fracture Mechanics, **41**, pp. 499-513, 1992.

[23] M. J. Caton, J. W. Jones, J. M. Boileau, and J. E. Allison, "The effect of solidification rate on the growth of small fatigue cracks in a cast 319-type aluminum alloy," Metallurgical and Materials Transactions, **30A**, pp. 3055-3068, 1999.

[24] J. M. Larsen, J. C. Williams, and A. W. Thompson, “Crack-closure effects on the growth of small surface cracks in Titanium-Aluminum alloys,” Mechanics of Fatigue Crack Closure, ASTM STP 982, ASTM, pp. 149-167, 1988.

[25] J. M. Larsen, J. R. Jira, and K. S. Ravichandran, “Measurement of small cracks by photomicroscopy: experiments and analysis,” Small Crack Test Methods, ASTM STP 1149, ASTM, pp. 57-80, 1992.

[26] S. K. Jha, M. J. Caton, and J. M. Larsen, "Mean vs. life-limiting fatigue behavior of a nickel-based superalloy," Superalloys 2008, TMS, pp. 565-572, 2008.

[27] M. Isida, T. Yoshida, and H. Noguchi, "Parallel array of semi-elliptical surface cracks in semi-infinite solid under tension," Engineering Fracture Mechanics, **39**, pp. 845-850, 1991.

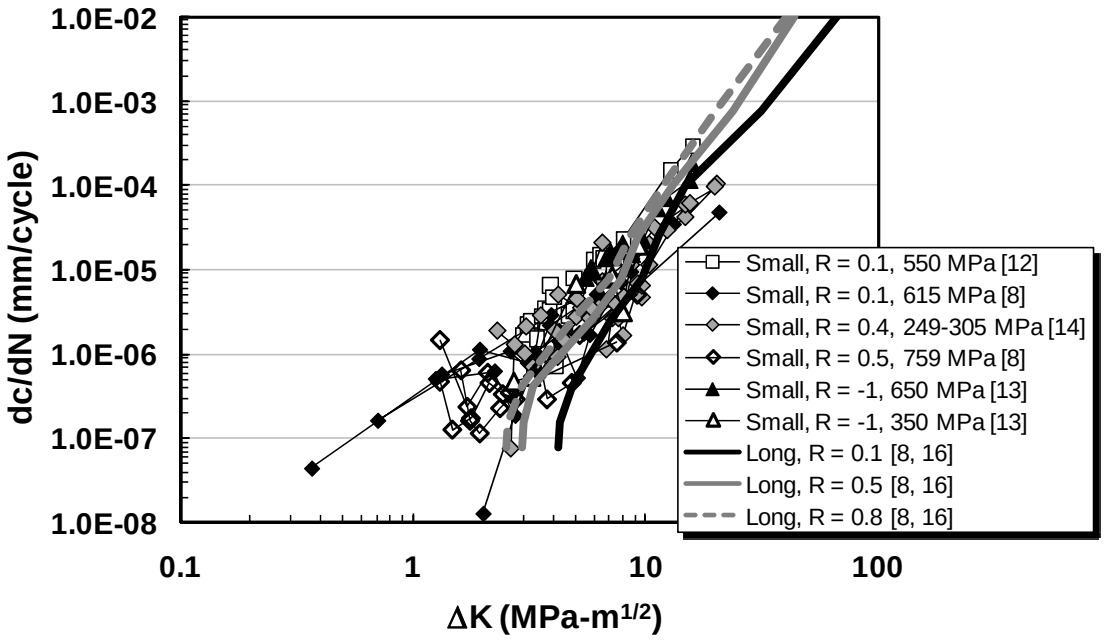

Fig. 1. A compilation of long and small fatigue crack growth data in Ti-6Al-4V acquired at several stress ratios and reported by numerous researchers [8, 12-14, 16].

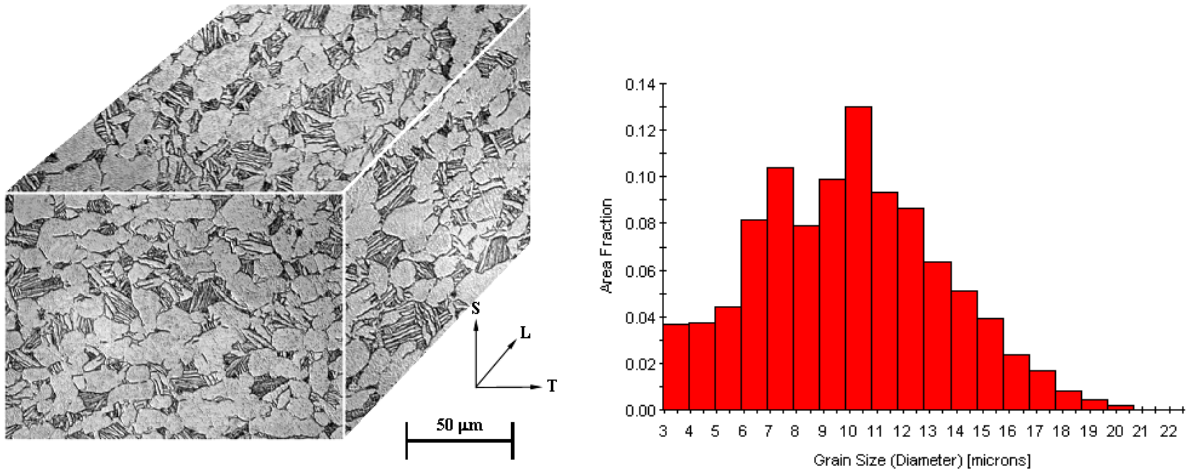

(a) (b)

Fig. 2. (a) Microstructure of the Ti-6Al-4V alloy examined [8]. (b) The primary alpha grain size distribution acquired through orientation image mapping (OIM) software.

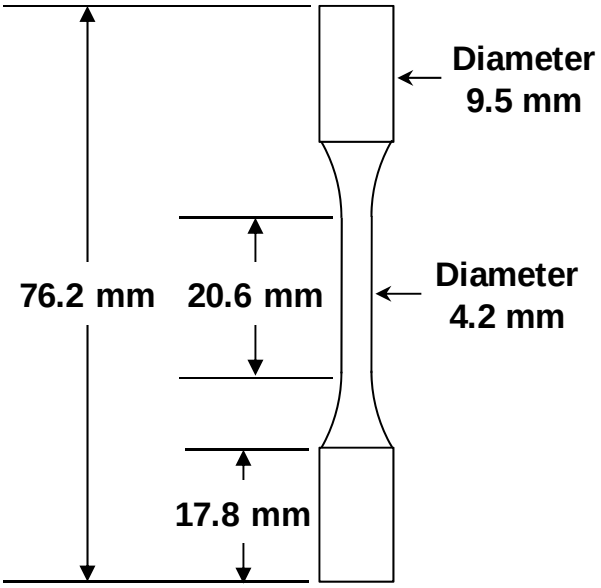

Fig. 3. The cylindrical fatigue specimen used to monitor small crack growth rates.

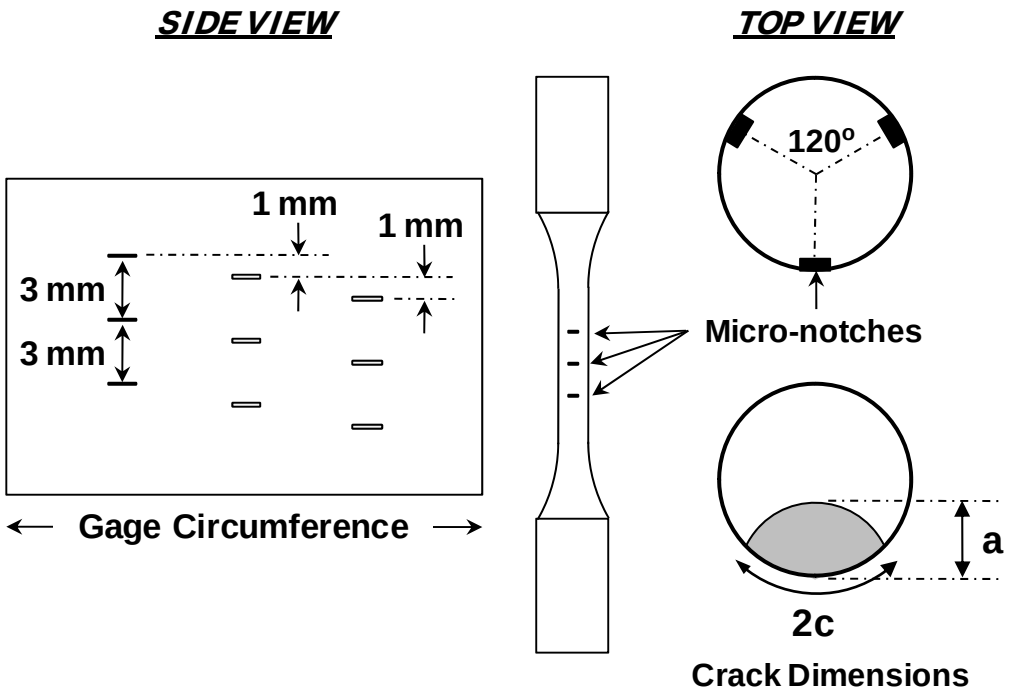

Fig. 4. Nine micro-notches were milled into each fatigue specimen using a focused ion beam (FIB) with the orientation shown above.

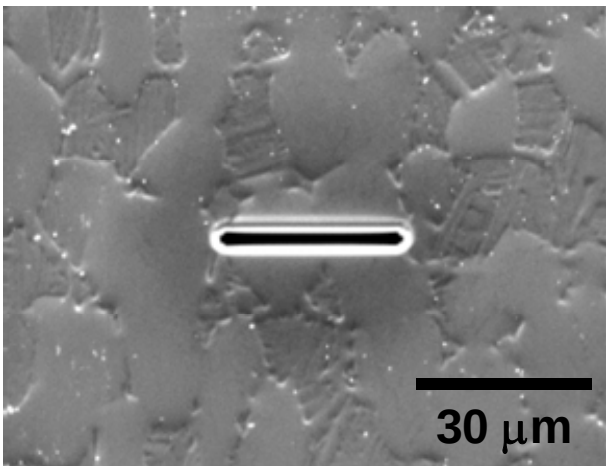

(a)

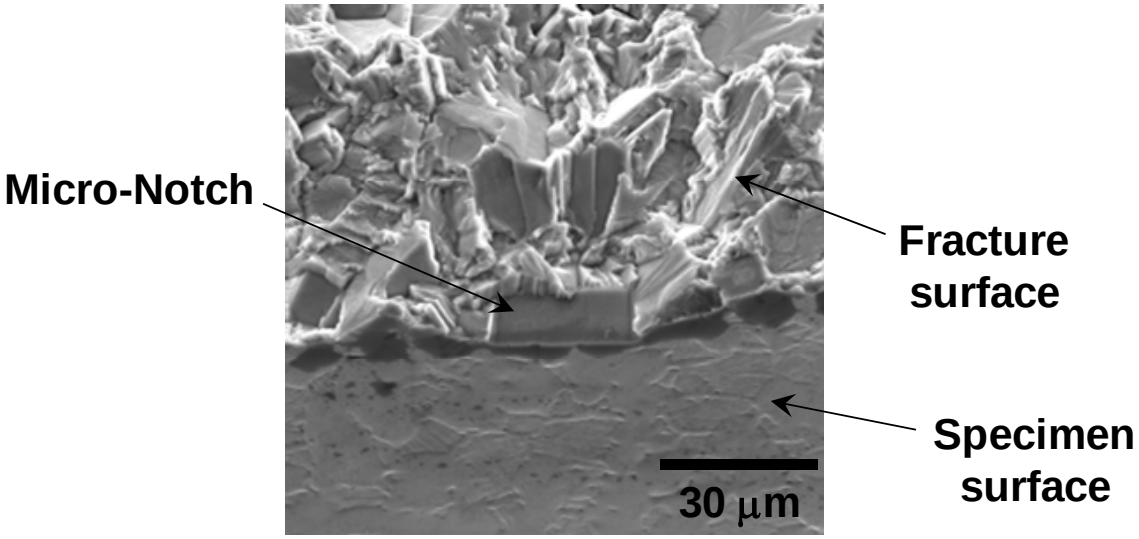

(b)

Fig. 5. An example a FIB-milled micro-notch as viewed with SEM images of (a) the side of the specimen and (b) the fracture surface of a tilted specimen.

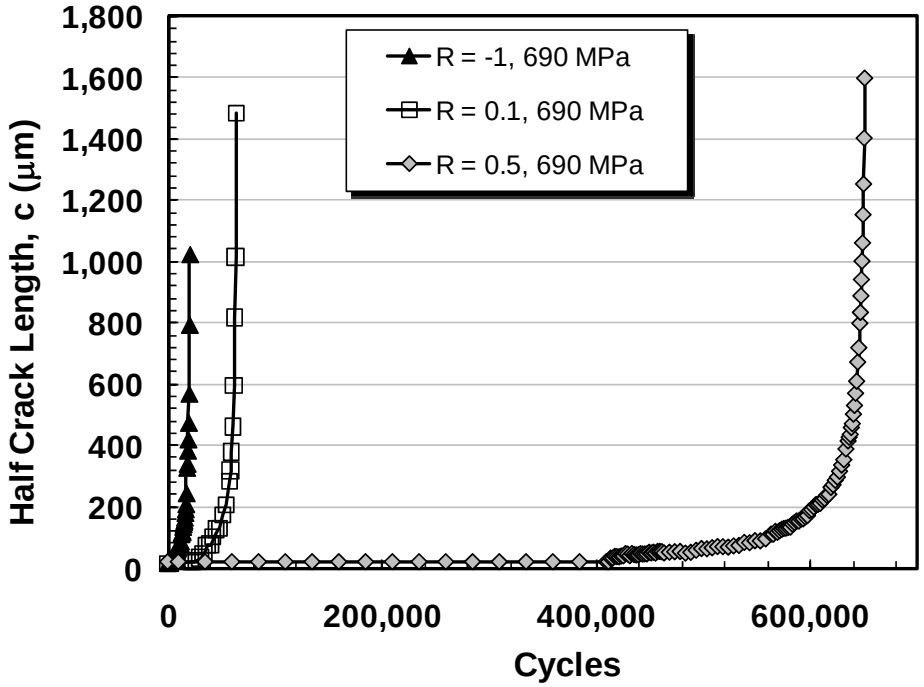

Fig. 6. Small crack size as measured with replication for the dominant crack in each of the specimens tested at σ_{max} = 690 MPa.

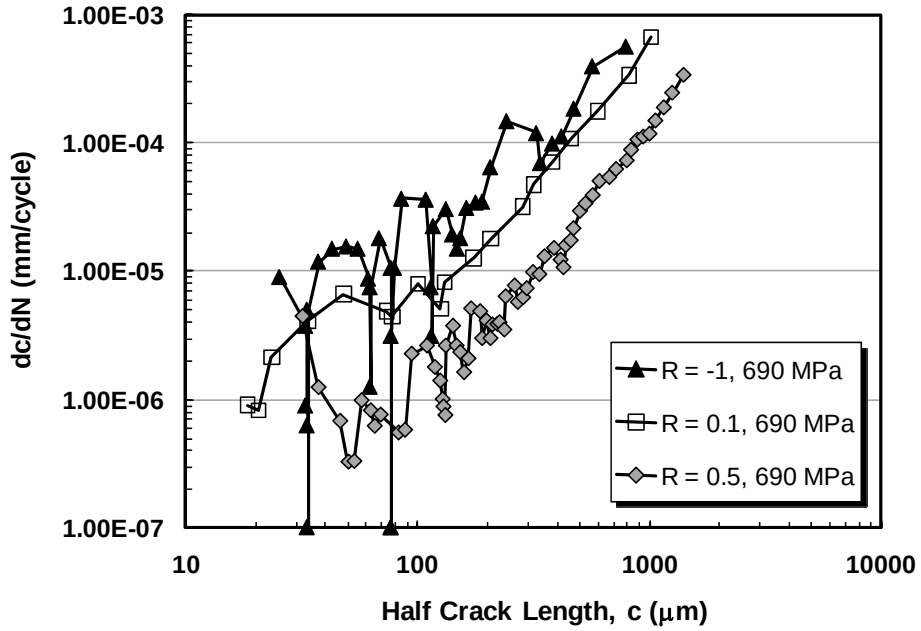

Fig. 7. Crack growth rate plotted as a function of crack size for the dominant crack in each of the specimens tested at σ_{max} = 690 MPa. Growth rates were determined by applying a 3-point sliding polynomial curve fit to the data shown in Fig. 6.

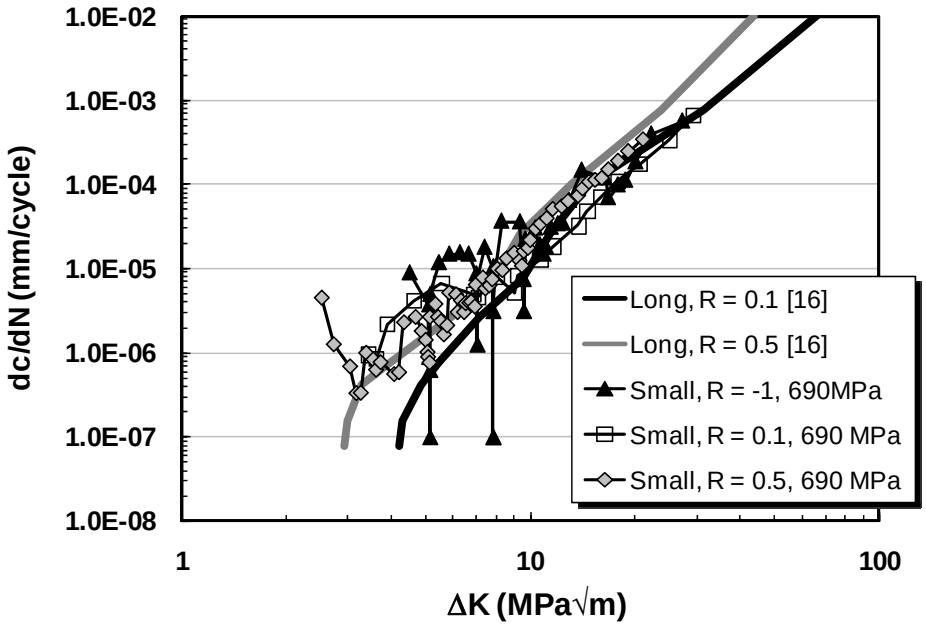

Fig. 8. Crack growth rate plotted as a function of ΔK for the dominant crack in each of the specimens tested at σ_{max} = 690 MPa. Growth rates were determined by applying a 3-point sliding polynomial curve fit to the data shown in Fig. 6.

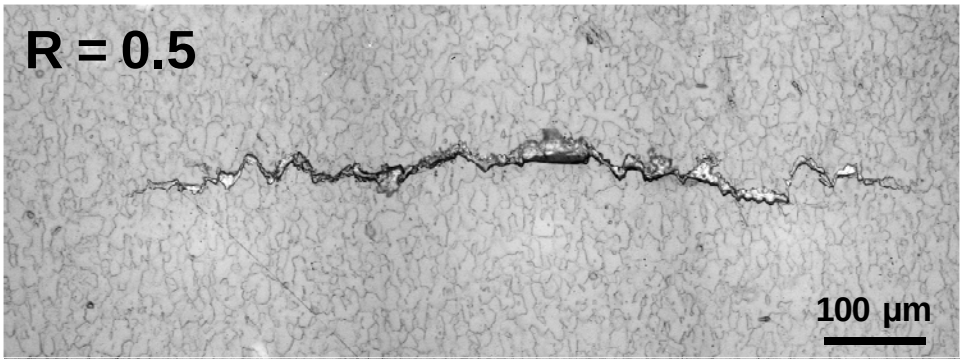

(a)

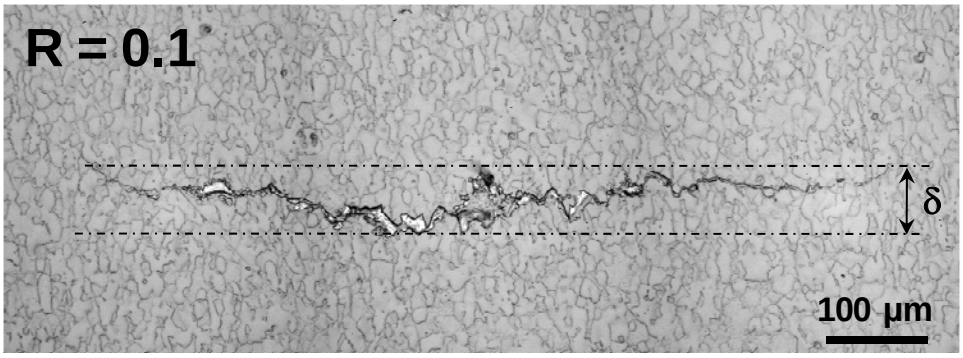

(b)

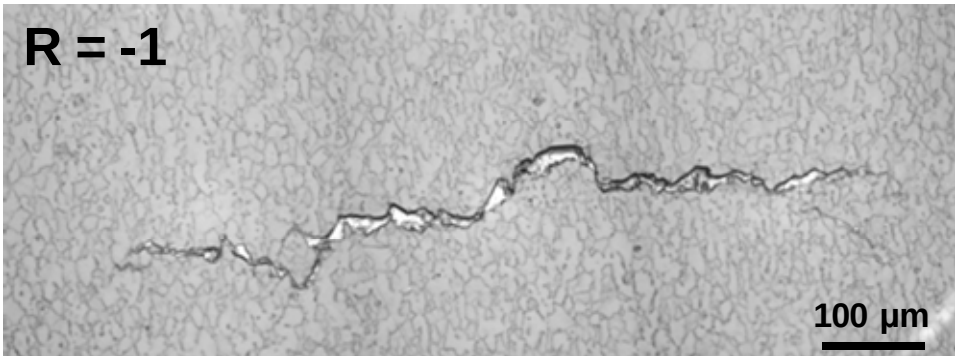

(c)

Fig. 9. Photos taken from the acetate replicas for the dominant small fatigue cracks grown at a maximum stress of 690 MPa and stress ratios of (a) R = 0.5, (b) R = 0.1, and (c) R = -1.

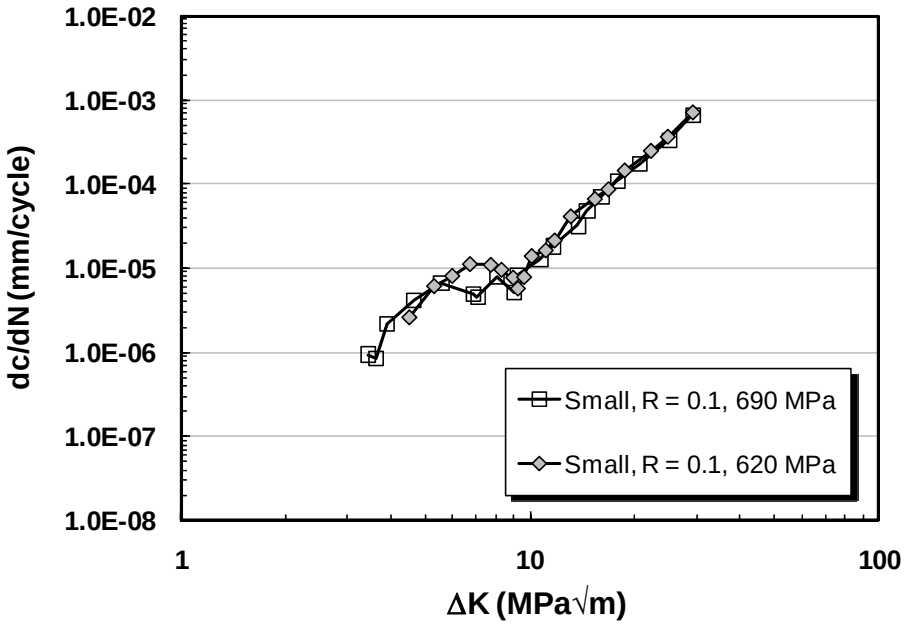

Fig. 10. The effect of stress level on small crack growth rates for a given stress ratio (R = 0.1).

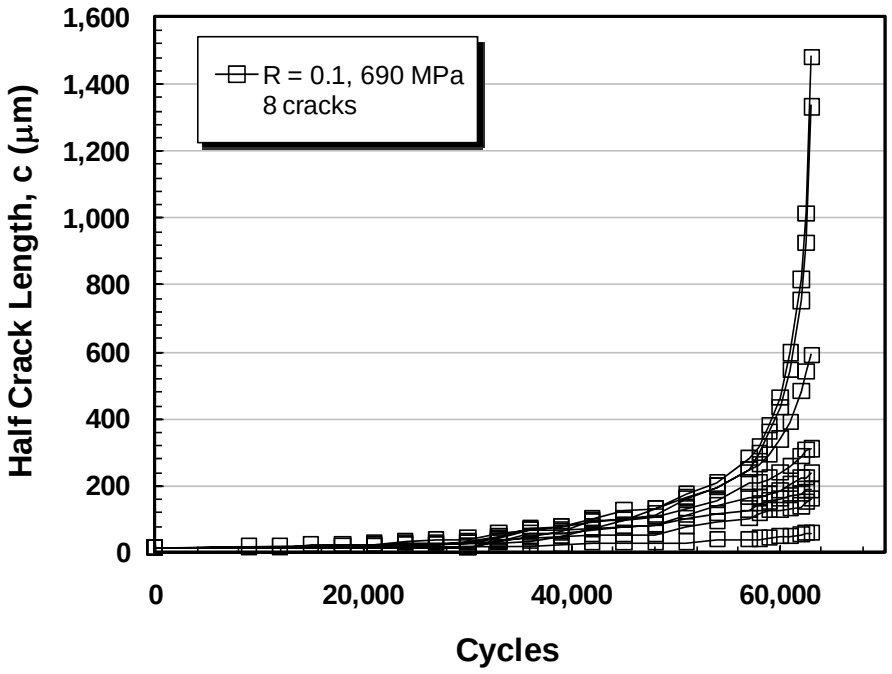

(a)

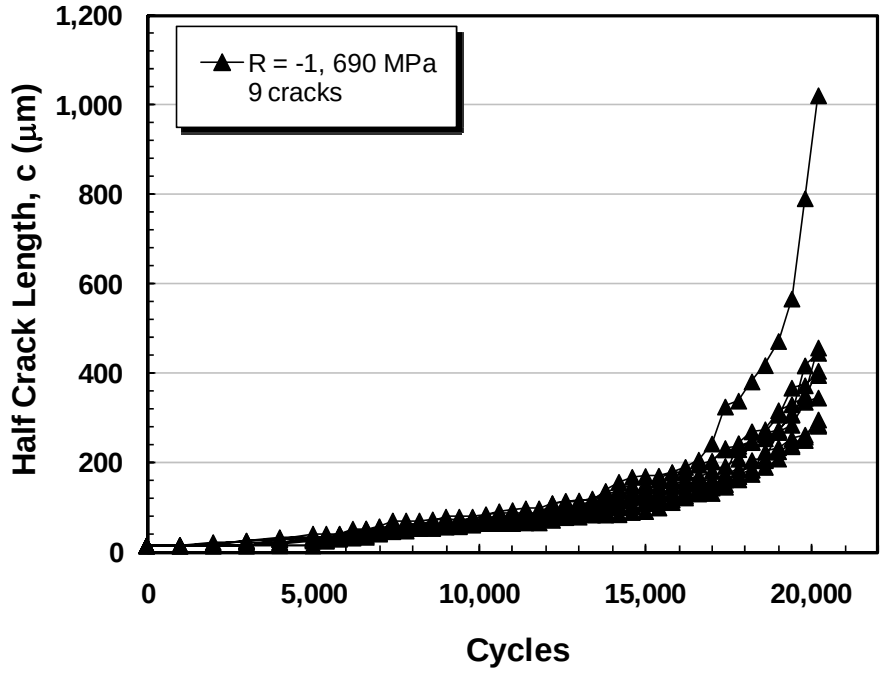

(b)

Fig. 11. Small crack size as measured with replication for all of the cracks that initiated from micro-notches in the specimens tested at σ_{max} = 690 MPa and (a) R = 0.1 and (b) R = -1.

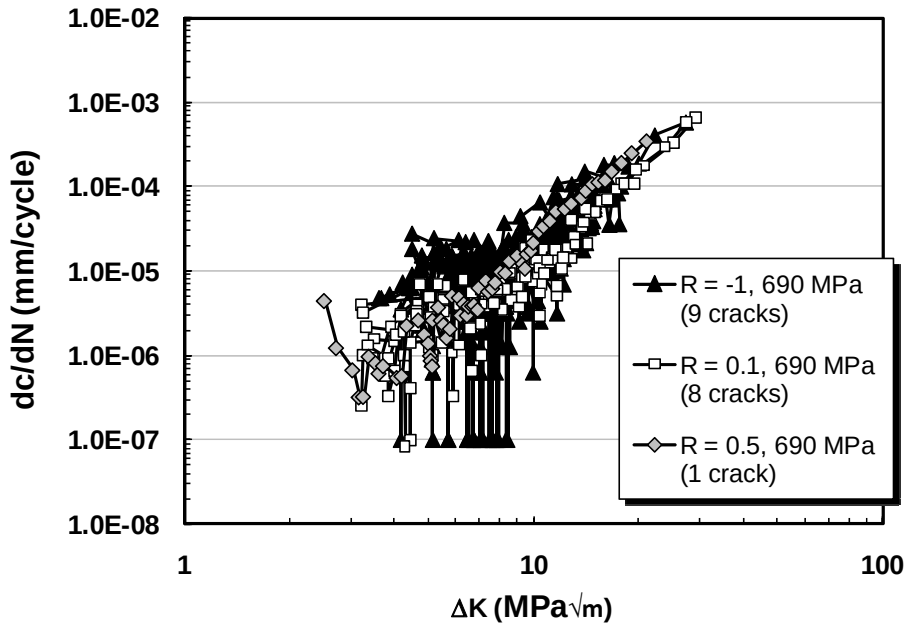

Fig. 12. Small crack growth rates for all cracks that initiated from micro-notches at σ_{max} = 690 MPa and stress ratios of 0.5, 0.1, and -1.

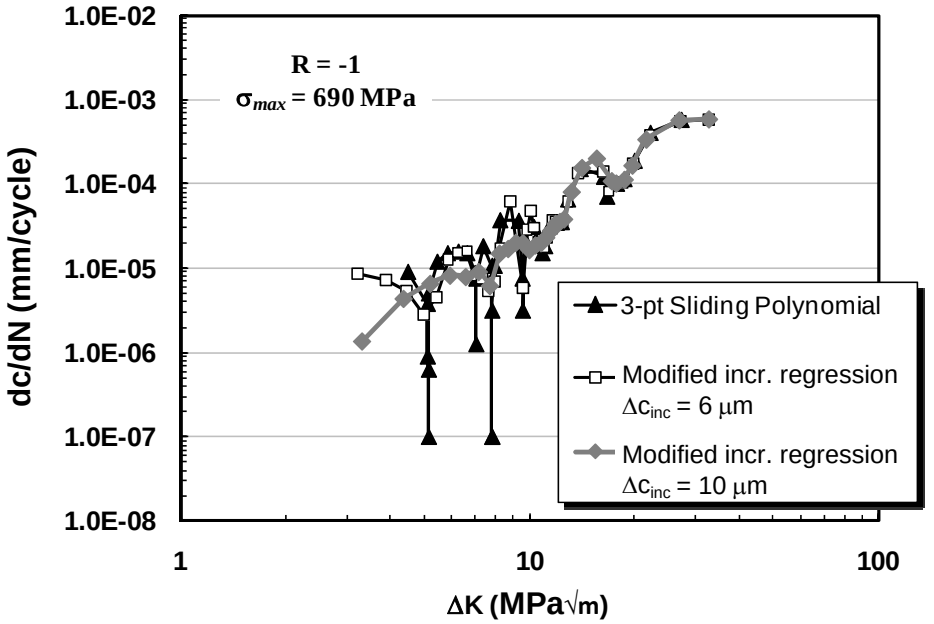

Fig. 13. Small crack growth rates for the dominant crack grown at σ_{max} = 690 MPa and stress ratio of -1, with three different regression methods.

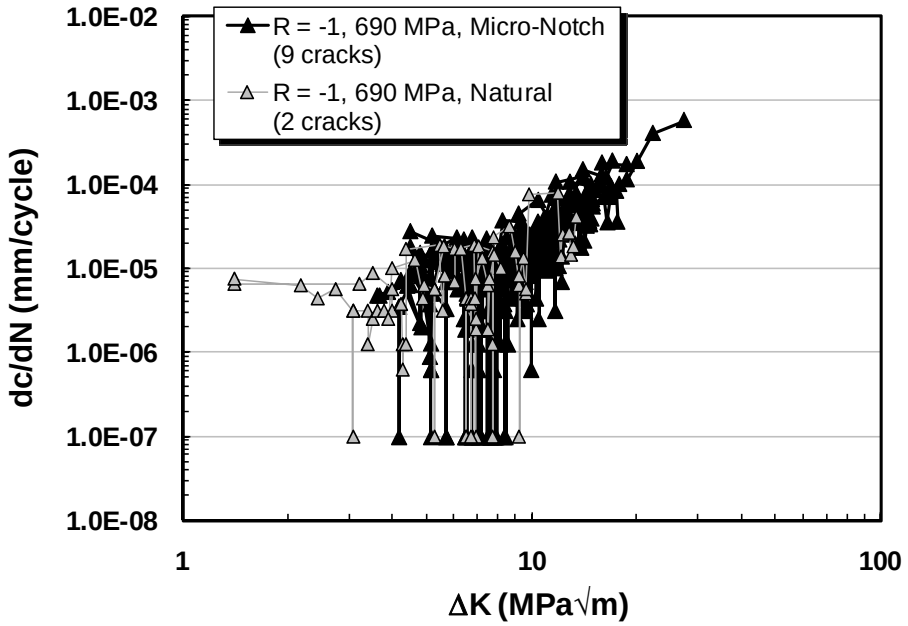

Fig. 14. Crack growth rates for small cracks grown at σ_{max} = 690 MPa and stress ratio of -1, initiating naturally and from micro-notches.

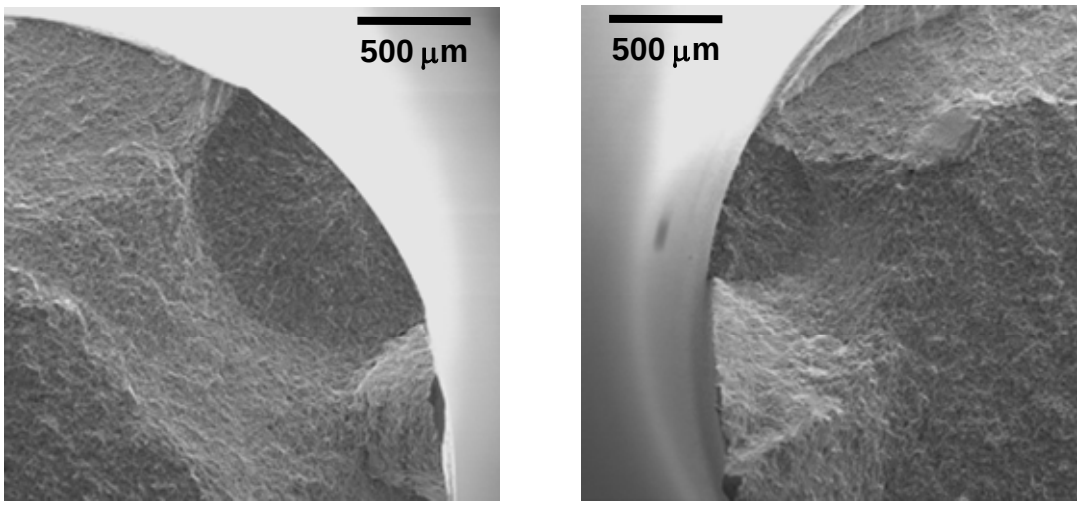

(a) (b)

Fig. 15. SEM images of small cracks on the fracture surface of the specimen tested at σ_{max} = 690 MPa and R = 0.1. The aspect ratios for these cracks were measured to be (a) a/c = 1.03 and (b) a/c = 1.15.

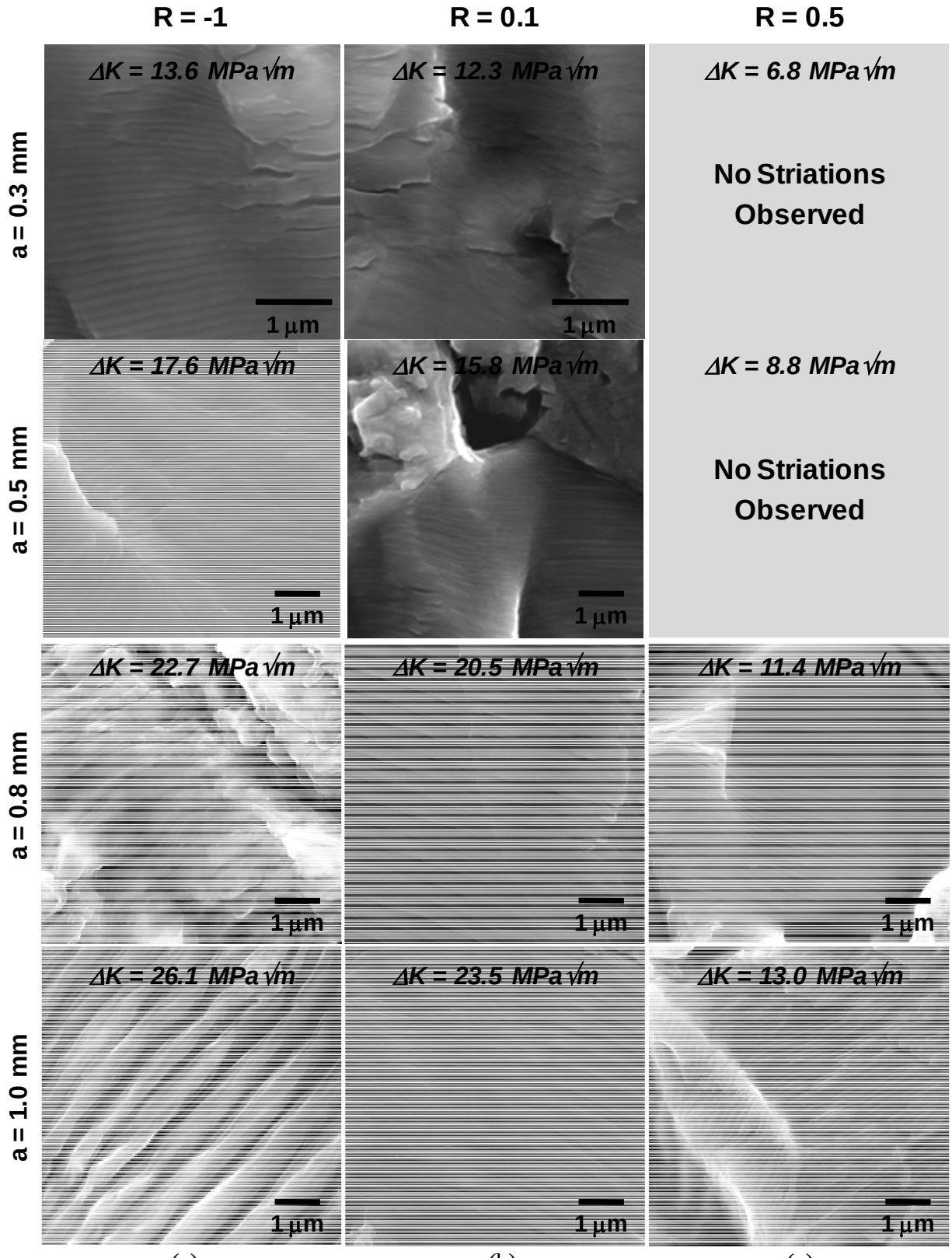

Fig. 16. SEM images of fatigue striations on the fracture surfaces of the specimens tested at σ_{max} = 690 MPa and (a) R = -1, (b) R = 0.1, and (c) R = 0.5.

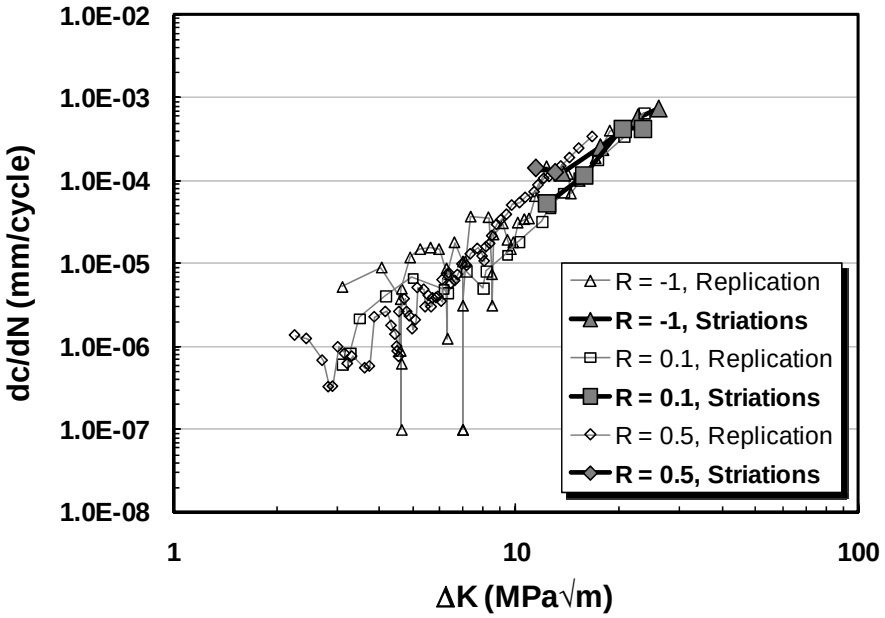

Fig. 17. Small crack growth rates calculated from striation spacing measurements compared to data generated from measurements of surface replicas.